Micro-interferometry for Measurement of Thermal Displacements at Fiber/Matrix Interfaces

by N.R. Sottos, W.R. Scott and R.L. McCullough

ABSTRACT—A micro-interferometric technique for measuring out-of-plane thermal displacements on a scale commensurate with the dimensions of the fiber/matrix unit cell is described. A scanning micro-interferometer is used to image surface displacements of samples containing a single-pitch-based carbon fiber embedded in an epoxy matrix. The interferometer design gives the necessary resolution to detect small changes in thermal displacements in the fiber/matrix interface region. The samples were heated electrically through the fiber to create radially symmetric temperature and displacement fields. Repeatable displacement measurements were obtained on a radial line across the interface region with an accuracy of ±25Å. A sharp expansion of the matrix surrounding the fiber was observed with each heating. Overall, the experiments demonstrate the utility of micro-interferometry for measuring submicron displacements.

Introduction

Many of the overall thermomechanical properties of a composite material are influenced by the local structure and properties of a region developed at the fiber/matrix interface. Controlling and optimizing the properties of this interface region are highly desirable for enhanced performance of the composite. In order to develop and evaluate mechanics models or empirical relations which correlate composite behavior with interface behavior, the properties of the interface region must be accurately measured. There is, however, a lack of adequate experimental techniques for quantitatively determining material properties and behavior in a region of this size. Consequently, there is increased interest in refining the scale of micromechanical measurements to include the interfacial region.

Most of the reinforcing fibers used in composite materials have diameters ranging from 5 μm to 150 μm, while the distance between fibers for a high volume fraction is on the order of 2 μm or less. Thus, any experimental technique for measuring *in situ* mechanical behavior in the interface region must have a spatial resolution commensurate with the dimensions of the fiber/matrix unit cell. Cox, Morris and James[1] have reported one method for high sensitivity, high spatial resolution strain measurements around fibers in composite alloys. The technique enables the measurement of relative in-plane displacement fields using stereo-imaging of SEM micrographs. The displacements are determined by comparing the position of visible surface features on stereo micrographs taken before and after a load is applied. The displacement sensitivity of this instrument is reported as ±20 Å when using SEM images. This method has been employed to study local thermal fatigue near the fiber/matrix interface.[2] Additionally, Morris, Inman and Cox[3] have used this technique to measure out-of-plane displacements between fiber clusters in heated unidirectional graphite/epoxy composites. The spatial resolution of the apparatus in this work is reported to be about 1 μm while the net error in the displacements is ±75 Å. An increased displacement sensitivity of ±10 Å is reported in a more recent work,[4] where digital image processing is used to replace manual stereoscopic analysis for the measurement of small strains.

Previous studies by Scott *et al.*[5,6] and Huber *et al.*[7] have demonstrated the utility of heterodyne micro-interferometry for measurement of submicron displacements caused by ultrasonic waves propagating at frequencies of one megahertz and above. Because an interferometer probe is a light beam, it has the capability to resolve small displacements in regions comparable to the wavelength of the light being used. In this paper, a micro-interferometric technique is described for measuring thermal displacements with an out-of-plane resolution of 50 Å and a potential in-plane resolution of 1.0 μm. The motivation behind the development of an interferometer with this resolution has been to provide a technique for accurately measuring deformations in the interface region. The interferometer is used to image the out-of-plane thermal displacements of specimens consisting of a single 30-μm carbon fiber embedded in an epoxy matrix. Details of the apparatus, the heating mechanism, sample preparation, and the displacement measurements will be described. Results showing the differential thermal displacements of the fiber and matrix are presented.

N.R. Sottos is Assistant Professor, University of Illinois, 216 Talbot Laboratory, 104 S. Wright Street, Urbana, IL 61801. W.R. Scott is Group Leader, Naval Air Development Center, Code 6063, Warminster, PA 18974. R.L. McCullough is Professor, University of Delaware, Department of Chemical Engineering, Newark, DE 19716.

Apparatus

The current design for a scanning heterodyne micro-interferometer has evolved from a number of previous designs reported in the literature by Scott *et al.*[5,6] A distinguishing feature of these earlier methods is the formulation of a magnified image on the face of a scanning detector, while the sample serves as a stationary mirror in one arm of the interferometer. By using a scanning detector window with a diameter smaller than the obtainable resolution of the image, detailed displacement contour plots can be made without the necessity for continuous realignment of the specimen. This general technique is also employed in the current interferometer described below. Additionally, a more detailed description of the interferometer is given by Ryan *et al.*[8]

A schematic diagram of the scanning heterodyne micro-interferometer developed for this study is shown in Fig. 1. A single, linearly polarized light beam of wavelength 514.5 nm from an Argon laser is incident upon a 40-MHz acousto-optic modulator (AOM) producing two beams which are sent along different arms of the interferometer. The first beam, or reference beam, is directed along path A in Fig. 1 and propagates with the same frequency as the beam incident upon the AOM. The second beam, which follows path B in Fig. 1, is shifted in frequency by 40 MHz and is used to illuminate the sample surface. Hence, the sample serves as a mirror in this arm of the interferometer. The sample is mounted on a translation and rotation stage, such that only the outer edges of the back face of the sample are actually touching the fixture. This arrangement allows the sample to displace freely. The sample is manually adjusted for angular tilt when aligning the interferometer.

The combination of the polarizing cube and the quarter wave plate ($\frac{\lambda}{4}$) allows the sample to be illuminated at normal incidence without excessive light loss. The polarizing cube reflects vertically polarized light, and transmits horizontally polarized light. The vertically polarized light incident upon the cube is reflected through the quarter-wave plate, which circularly polarizes it. After reflection from the sample, the beam passes back through the quarter-wave plate, producing a horizontally polarized beam that passes through the cube toward the beam splitter. The half-wave plate ($\frac{\lambda}{2}$) in the reference arm rotates the polarization of the unmodulated beam to match the beam from the sample arm. The two beams are then recombined at the beam splitter.

The combined beams arrive at the primary lens of a QUESTAR long-distance microscope. The sample surface being imaged lies within the object plane of the microscope. An image is formed behind the microscope and is magnified onto the image plane of a scanning photodiode detector using an eyepiece lens. Through the use of different lenses, magnifications from $1\times$ to $100\times$ are possible. Light intensity may drop below acceptable levels with magnifications of greater than $100\times$, making it difficult to achieve the potential transverse resolution of 1 μm. Depending on the magnification of the image, the in-plane resolution is either limited by the optical system or by the diameter of the detector window. At present, the detector window is 0.75 mm in diameter, which, at a magnification factor of $85\times$, yields an in-plane resolution of approximately 9 μm.

If there is a sharp change in the phase data, it is averaged across the window. Rapid spatial phase fluctuations of greater than 2π could in principle lead to phase and displacement ambiguities. The use of polished specimens makes this type of error highly unlikely in these experiments. However, in areas where steep surface gradients exist, time-dependent displacements are monitored during heat up and cool down to confirm that no 2π discontinuities are missed.

The large effective numerical aperture (~ 0.6) of the long-distance microscope increases light-gathering power and permits high-resolution imaging. It incorporates a 20.3-cm (8-in.) diameter primary mirror, and operates with a working distance of 30 to 55 cm. Consequently, the device allows a reasonable working distance without the need for position detectors to avoid sample contact, as is necessary for other high magnification devices. The shortest working distance of 30 cm was used for the current experiments.

One corner of the image plane is reflected by a mirror onto a second photodetector. The signal at this stationary photodetector is used as a phase reference signal. As the scanning photodetector moves across the image, the phase of the image signal is compared to the phase of the reference signal. As a result, dynamic disturbances, such as air turbulence, mechanical vibration, and thermal drift, that occur within the interferometer but away from the

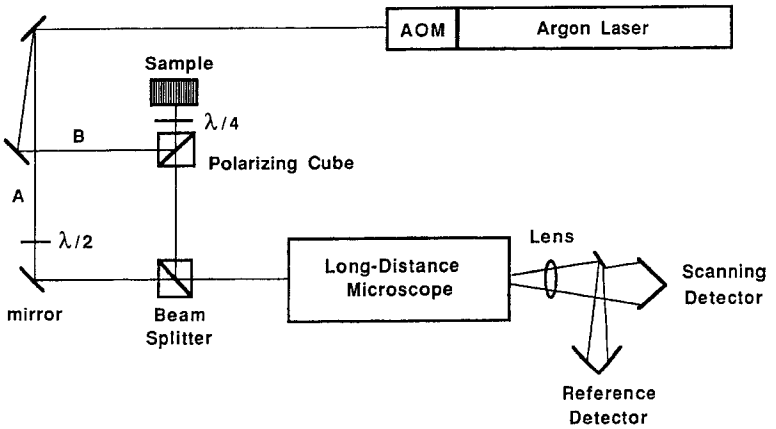

Fig. 1—Schematic of scanning micro-interferometer

sample do not affect the measurements. The light that forms the sample image differs in frequency by 40 MHz from the light that forms the reference image. Any z-axis displacement of the sample surface will produce phase shifts in the 40-MHz beat signal arriving at the photodetector. This arrangement allows the sample to remain stationary while the detector is scanned across the sample image, alleviating the difficulty of having to focus a beam onto the surface of a moving specimen. The scan rate is slow enough to permit measurement of the phase shift using a high-frequency lock-in amplifier.

The interferometer system is shown in Fig. 2. The photodiode detector is moved across a specified x-y window on the magnified sample image in a raster pattern using a computer-controlled scanner. The servomotors of the scanner are capable of producing displacements in 0.1-μm steps and maintain their position accurate to 0.1 μm. The lock-in amplifier is used to compare the phase of the 40-MHz signals from both the reference and the scanning detectors. As the detector scans across the image, the lock-in amplifier produces a signal proportional to the phase. This output is monitored by a digital oscilloscope for which the sweep rate is synchronized to the scan, so that one scan line corresponds to one 1024-point waveform on the oscilloscope screen. After an entire scan line is displayed on the scope, it is stored on the microcomputer. The detector is then scanned across the next line of the window until the entire specified area has been covered.

Sample Preparation and Heating

The interferometer described above is used to image thermal displacements of specimens consisting of a single carbon fiber embedded in epoxy. A schematic of the specimen is shown in Fig. 3. The fibers used for this study are 30-μm pitch-base carbon fibers supplied by Textron. The manufacturer has specified these fibers to have a Young's modulus of 41 GPa and a slightly negative coefficient of thermal expansion ($\sim -0.5 \times 10^{-6}\,°C^{-1}$). All of the fibers are washed in isopropyl alcohol to remove any surface residues before being used in a specimen. For the matrix, a Shell EPON-828 epoxy resin with a PACM-20 curing agent is chosen. Properties of the neat resin are given in Table 1. The modulus, Poisson's ratio and thermal conductivity are obtained from the manufacturer, while the coefficient of thermal expansion has been determined from thermal mechanical analysis (TMA). Samples are made by placing a fiber into the center of a mold which is then filled with epoxy. All samples are held for one hour at 80°C to minimize the bubbles in the resin phase, then cured for 30 minutes at 150°C, and allowed to slow cool to room temperature overnight. The outer radius of the sample is 1.5875 cm, which is approximately 1000 times the radius of the fiber. Specimens are cut to a length of 2 cm and the front and back faces polished metallographically. Polishing of the front face on which the measurements are made is critical to insure a reflective surface.

To heat the sample, a small current of 11.0 mA is run through the fiber. Leads are attached to the front and back polished faces of the specimen as shown in Fig. 3. A thin layer of gold, approximately 1000-Å thick, is then sputtered onto the surface to provide both a current conduction path and a highly reflective surface across the circular cross section of the fiber/matrix interface. There are several advantages to heating the sample electrically in this manner. A repeatable, radial temperature field is generated in the sample which can be predicted analytically. The equilibrium time for heating and cooling the region of interest is small (typically less than ten seconds). Finally, there is minimal convection of heat into the interferometer path minimizing thermal effects on the apparatus.

Knowledge of the temperature distribution in the sample is critical in order to estimate the maximum temperature in the sample to avoid overheating the epoxy matrix. To reproduce or model the experiment, it is also necessary to know the temperature profile. Analytical prediction of the temperature distribution in the sample is straightforward and given in the appendix. After substituting the appropriate material properties into eq (4) in the appendix, the analytical temperature distribution in the sample is calculated. A power input of $P = 68.0$ mW is used to heat the samples. Figure 4 is a plot of the predicted steady-state temperature change in the sample as a function of radial distance. The temperature in the fiber is nearly constant, while the matrix temperature decreases rapidly away from the interface.

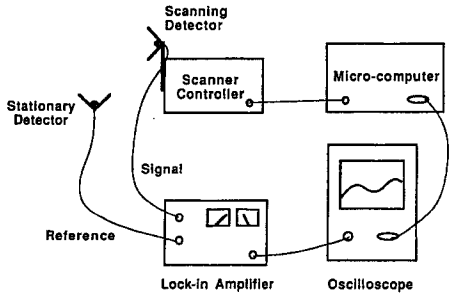

Fig. 2—Schematic of experimental apparatus

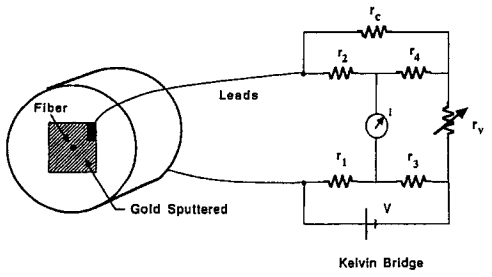

Fig. 3—Schematic of single-fiber specimen connected in a Kelvin bridge

TABLE 1—MATRIX MATERIAL PROPERTY VALUES

Property	Shell EPON 828 Resin
E (MPa)	2.5
α ($\times 10^{-6}\,°C^{-1}$)	68.0
K_m ($\frac{W}{m\,°C}$)	0.18
ν	0.33

In addition to analytical predictions, an experimental measurement of the fiber temperature was obtained by monitoring the change in resistance of the fiber when it was heated. The leads on the front and back faces of the sample were connected in a Kelvin bridge as shown in Fig. 3. The bridge was balanced by adjusting the variable resistor. A low d-c voltage of 0.75 V was applied across the bridge so that it could be balanced. Any heating which occurred from this low power input was negligible. A small change in the sample resistance caused an imbalance in the current across the bridge which was initially set to zero. The change in bridge current was calibrated with the temperature of the fiber by placing the sample in an oven and recording the bridge current after the sample temperature reached equilibrium. Measurements were collected for several temperatures (at increments between 19-42° C). The linear calibration curve shown in Fig. 5 was obtained.

When measuring thermal displacements, the bridge current was monitored, and the corresponding fiber temperature during the experiment was determined using the calibration curve. Although the calibrations were performed for temperatures lower than heated to in the experiment, a linear fit of the curve was extrapolated approximately 20° C to the desired temperature range. The experimental fiber temperature determined from the bridge calibration was compared to the analytic prediction for a range of values of input power. Figure 6 is a plot comparing the theoretical and experimental fiber temperatures. The slopes of the two curves differ by six percent. At P = 68.0 mW, the analytical value for fiber temperature is 45° C and the experimental value is 47° C. Hence, the two estimates of the fiber temperature during the experiment differ by less than five percent.

Experiment and Results

To measure the net thermal displacements of the sample, an unheated scan of the surface must be made initially. The sample is then heated and a second scan is run. During each scan, phase data are continuously recorded and stored. Displacements are then calculated by subtracting the phase data of unheated scan lines from the heated ones. For this particular interferometer, 360 deg of phase change corresponds to a distance of 0.257 μm. All out-of-plane displacements are measured relative to the same reference point which lies off the scan over 30-fiber radii from the fiber center.

Figure 7 is a contour plot of the unheated fiber and surrounding matrix region. A window of 5.0 × 3.8 mm was scanned at a rate of 0.2 mm/s on an 85× magnified image of the interface region. This window corresponds to a 59 × 45-μm field on the sample surface. During the scan, the laser power was held steady at 500 mW. Although the surface of the specimen was carefully polished, the interferometer has a high enough out-of-plane sensitivity

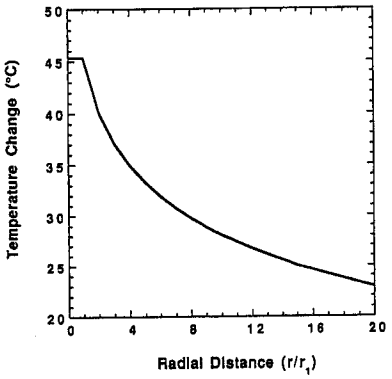

Fig. 4—Analytical steady-state temperature profile as a function of radial distance in the sample

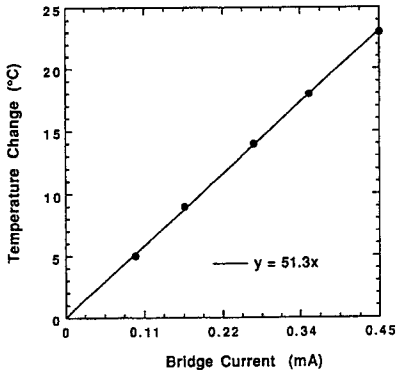

Fig. 5—Calibration curve of bridge current versus fiber temperature

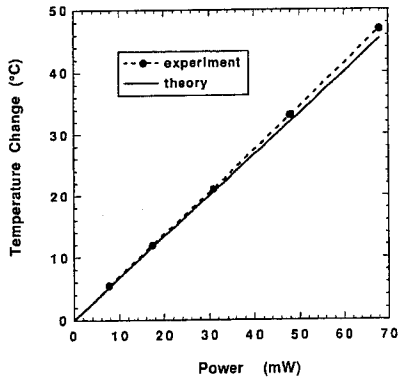

Fig. 6—Comparison of theoretical and experimental fiber temperatures versus power input to the sample

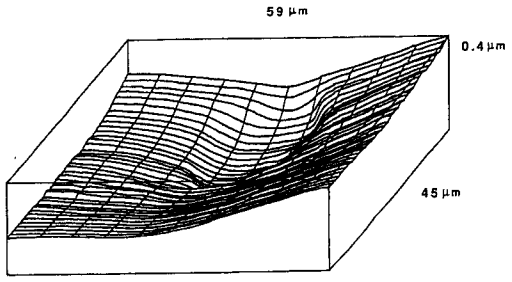

Fig. 7—Contour plot of initial unheated sample surface magnified 85×

to reveal the topology of the surface before heating. In fact, the fiber was slightly depressed below the surface of the surrounding matrix. The epoxy matrix has a tendency to absorb moisture and is believed to have swelled up around the fiber. This swelling is small, however, as the distance between the highest and lowest portion of the scan is only 0.40 μm.

To heat the specimen, a d-c voltage of 12 V is applied across the Kelvin bridge causing a net power of 68 mW to be delivered to the fiber. As the sample is heated, the surface undergoes a positive displacement and the phase output monitored on the oscilloscope at any point in the scan window is seen to increase as expected. The sample comes to thermal equilibrium within ten seconds. Equilibrium is determined as the point when the phase of the heated sample is no longer changing with time.

To measure the thermal displacements at the interface, it was convenient to make measurements on single scan lines extending across the fiber center. The magnification of the interferometer was decreased to 25× for these measurements so that more of the far-field matrix could be included in the scan. Because the scanners have a limited range of motion, the magnification has to be reduced to scan over a larger portion of the sample surface. Figure 8 is a plot of the raw data from the unheated and heated scans of the surface. Heating the sample caused the matrix to expand upwardly and pull the fiber with it. Subtraction of the initial unheated scan line from the heated scan line yields the net thermal displacement of the region. In Fig. 9, the experimental thermal displacements are plotted as a function of radial distance from the fiber center ($r = 0$). Displacements have been normalized by subtracting from each point the value of the displacement at a point 30-fiber radii out. The displacement of the fiber is nearly constant. However, there is a sharp rise in the displacement of the matrix near the interface, which peaks at about 5-fiber radii out. After this point, the matrix displacements decrease somewhat linearly with radial distance.

A final scan of the region is made after the voltage is removed from across the bridge and the sample is cooled. Subtraction of the two unheated scans, as shown in Fig. 10, produces random fluctuations about a horizontal line corresponding to zero displacement. The nature of these fluctuations appears to be digital. The accuracy of the measurements can be assessed by determining the average of the absolute values of the fluctuations from the zero line in Fig. 10. In this manner, the accuracy for the interferometric measurement of thermal displacements is approximately ±25 Å.

Series of displacement measurements were made on three samples. The repeatability of the measurement on the same sample was excellent. The data for two consecutive runs on each sample were then averaged together and compared across samples. The repeatability of the measurement across samples from the same batch was also excellent. Overall, the displacement profile in Fig. 9 was repeated for each sample tested.

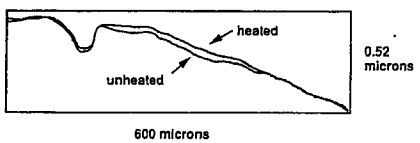

Fig. 8—Raw data from unheated and heated scan lines of sample surface

Discussion and Conclusions

An interferometric technique for accurately measuring deformations on a scale commensurate with the fiber/matrix unit cell has been developed. A scanning heterodyne micro-interferometer was designed with a potential transverse resolution of 1.0 μm and a normal resolution of 50 Å. Thermal displacements, as shown in Fig. 9, were successfully measured for specimens containing a single carbon fiber embedded in an epoxy matrix. The resolution of the interferometer is clearly high enough to detect the differential thermal displacements of the fiber and matrix due to the large difference in longitudinal coefficient of thermal expansion. Repeatable displacement measurements were recorded on each sample and across all three of the samples tested. The accuracy of the displacement measurements is approximately 50 Å. Thus, the apparatus can be used to detect small changes in thermal displacements near the fiber/matrix interface.

Electrically heating the sample through the fiber provides a method for repeatable generation of symmetric

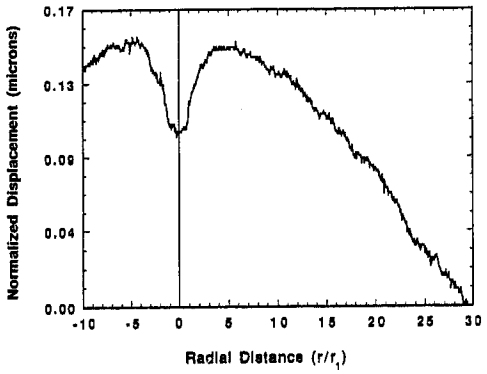

Fig. 9—Normalized out-of-plane thermal displacements as a function of radial distance from the fiber center

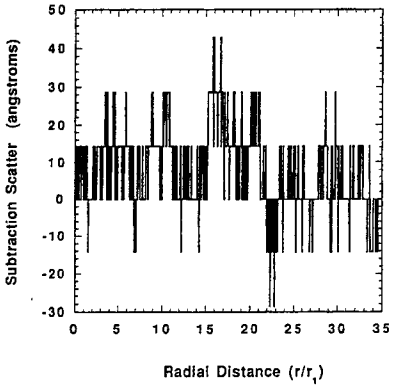

Fig. 10—Subtraction of two unheated scan lines yielding an average fluctuation of ± 25 Å about the horizontal line of zero displacement

displacement and temperature fields. By placing the sample in a Kelvin bridge and monitoring the change in resistance of the fiber, a reliable measurement of the fiber temperature is obtained. Theoretical predictions of fiber temperature compare well with the experimental values.

Previous studies of thermal displacements near the fiber/matrix interface[3] have found evidence of plastic behavior. Additionally, the matrix between clusters of three fibers has been observed to shrink rather than expand upon heating due to residual stresses from processing the material. None of these effects was observed in the current study. The cylindrical geometry of the single fiber sample allowed for a radially symmetric displacement field, free from the influence of other fibers. A repeatable expansion of the matrix surrounding the fiber was observed with each heating.

Overall, the utility of micro-interferometry for measurement of submicron thermal displacements is demonstrated. The ability to make such displacement measurements provides a quantitative method for studying material properties and behavior on a micro-scale. By using a single-fiber sample, the effects of any changes in the local properties of the interface region should be clearly observed. For example, the current displacement measurements can be compared to analytical predictions for a uniform matrix and for a matrix with nonuniform properties in an interface region. By fitting experimental data to theoretical predictions, trends in local material properties near the interface can be assessed. Prepared interfaces such as coatings can also be interrogated in this manner. In general, the out-of-plane measuring capability of this device lends it to many material-science applications where precise measurements of surface displacements are required.

Acknowledgments

This work was supported by an Office of Naval Research Fellowship and the Center for Composite Materials at the University of Delaware. The technical support and guidance of M.J. Ryan of APCOT Corp., and of Dr. S. Guceri at the Department of Mechanical Engineering, University of Delaware, as well as the interest and support of QUESTAR Inc. are greatly appreciated.

References

1. Cox, B.N., Morris, W.L. and James, M.R., "High Sensitivity, High Spatial Resolution Strain Measurements in Composites and Alloys," Proc. Nondestr. Test. and Eval. of Advanced Mat. and Comp. Conf., 25-39 (1986).

2. Morris, W.L. and Cox, B.N., "Thermal Fatigue of Unidirectional Graphite Composites," Proc. 6th Int. Conf. on Comp. Mat., ed. F.L. Matthews, N.C.R. Buskell, J.M. Hodgkinson, and J. Morton, 4, 344-352 (1987).

3. Morris, W.L., Inman, R.V. and Cox, B.N., "Microscope Deformation in a Heated Unidirectional Graphite-epoxy Composite," J. Mat. Sci., 24: 199-204 (1989).

4. James, M.R., Morris, W.L. and Cox, B.N., "A High Accuracy Automated Strain Field Mapper," EXPERIMENTAL MECHANICS, **20** *(1), 60-67 (March 1990).*

5. Scott, W.R., Huber, S. and Ryan, M., "An Image Scanning Heterodyne Microinterferometer," Rev. of Progress in Quantitative Nondestr. Eval., Plenum Press, New York, **7B**, *1065-1073 (1988).*

6. Scott, W.R., Ryan, M.J., Granata, D.M. and Sottos, N.R., "Nondestructive Evaluation and Characterization of Composite Materials Microinterferometry," 1st Navy Independent Research/Independent Exploratory Development Symp., CPIA Publication 492, **1**, *481-491 (1988).*

7. Huber, S., Scott, W.R. and Sands, R., "Detection and Analysis of Waves Propagating in Boron/Aluminum Composite Materials," Rev. Progress in Quantitative Nondest. Eval., Plenum Press, New York, **6B**, *1065-1073 (1987).*

8. Ryan, M.J., Scott, W.R. and Sottos, N.R., "Scanning Heterodyne Micro-interferometry for High Resolution Contour Mapping, Rev. of Progress in Quantitative Nondest. Eval., Plenum Press, New York (1990).

9. Carslaw, H.C. and Jaeger, J.C., Conduction of Heat in Solids, Oxford Science Publications, New York (1959).

Appendix

Analytical prediction of the temperature distribution in the sample requires the solution of the heat conduction equation in a finite composite cylinder, $-l \le z \le l$. The fiber, $0 \le r \le r_1$, which is heated by electric current, has thermal conductivity k_f. The matrix, $r_1 \le r \le r_2$, has thermal conductivity k_m. The governing equation for the temperature distribution in the fiber can be expressed as

$$\nabla^2 T = -\frac{P}{l\omega k_f} \tag{1}$$

and in the matrix as

$$\nabla^2 T = 0 \tag{2}$$

where P is the power input, l the specimen length, and ω the cross-sectional area of the sample face. Heat losses from the outer surfaces of the sample $r = r_2$ and $z = \pm l$ are neglected and assumed to be maintained at $T = 0$. At the fiber/matrix interface, $r = r_1$, the boundary condition can be expressed as[9]

$$k_f \frac{\partial^2 T}{\partial z^2} + \frac{2k_m}{r_1}\frac{\partial T}{\partial r} + \frac{P}{l\omega} = 0 \tag{3}$$

This condition assumes that there is no temperature discontinuity between the fiber and the matrix. Solution of eqs (1) and (2) yields the following steady-state temperature field in the sample.[9]

$$T(r,z) = \sum_{n=1}^{\infty} [A_n I_0(\varkappa_n r) + B_n K_0(\varkappa_n r)] \cos(\varkappa_n z) \tag{4}$$

where

$$A_n = Z_n K_0(\varkappa_n r_2) \tag{5}$$

$$B_n = -Z_n I_0(\varkappa_n r_2) \tag{6}$$

The constants Z_n are determined by the application of the boundary condition at $r = r_1$ and are given by

$$Z_n = \frac{-4P}{n\pi\omega l}\left[\frac{\sin\left(\frac{n\pi}{2}\right)}{\left(\frac{2k_m \varkappa_n E_1}{r_1}\right) - k_f \varkappa_n^2 F_0}\right] \tag{7}$$

where

$$F_0 = K_0(\varkappa_n r_1) I_0(\varkappa_n r_2) - I_0(\varkappa_n r_1) K_0(\varkappa_n r_2) \tag{8}$$

$$F_1 = I_1(\varkappa_n r_1) K_0(\varkappa_n r_2) + K_1(\varkappa_n r_1) I_0(\varkappa_n r_2) \tag{9}$$

The functions, I_0, I_1 and K_0, K_1 are modified Bessel functions of the first and second kind, respectively. The $\varkappa_n$ are the eigenvalues and are expressed as

$$\varkappa_n = \frac{n\pi}{2l} \tag{10}$$